DOT/FAA/AR-95/75

Office of Aviation Research
Washington, D.C. 20591

Engineering Approach to Damage Tolerance Analysis of Fuselage Skin Repairs

November 1996

Final Report

This document is available to the U.S. public through the National Technical Information Service, Springfield, Virginia 22161.

U.S. Department of Transportation
Federal Aviation Administration

NOTICE

Technical Report Documentation Page

1. Report No.	2. Government Accession No.	3. Recipient's Catalog No.
DOT/FAA/AR-95/75		

4. Title and Subtitle	5. Report Date
ENGINEERING APPROACH TO DAMAGE TOLERANCE ANALYSIS OF FUSELAGE SKIN REPAIRS	November 1996
	6. Performing Organization Code

7. Author(s)	8. Performing Organization Report No.
J.G. Bakuckas, Jr.[1], C.C. Chen[2], J. Yu[2], P.W. Tan[1], and C.A. Bigelow[1]	

9. Performing Organization Name and Address	10. Work Unit No. (TRAIS)
1 Federal Aviation Administration William J. Hughes Technical Center Atlantic City International Airport, NJ 08405 2 McDonnell Douglas Aerospace 1510 Hughes Way Long Beach, CA 90810	11. Contract or Grant No.

12. Sponsoring Agency Name and Address	13. Type of Report and Period Covered
U.S. Department of Transportation Federal Aviation Administration Office of Aviation Research Washington, D.C. 20591	Final Report
	14. Sponsoring Agency Code AAR-433

15. Supplementary Notes

FAA William J. Hughes Technical Center COTR: J. G. Bakuckas, Jr.

16. Abstract

A simplified approach to damage tolerance analysis of riveted fuselage skin repairs has been incorporated in a new user-friendly software package, Repair Assessment Procedure and Integrated Design (RAPID). In this study, the damage tolerance analysis methodology in RAPID was evaluated in terms of the fastener loads, stress-intensity factor solutions, crack growth, residual strength, and inspection schedule. Three example problems, each representing a typical fuselage skin repair configuration, were analyzed. The analysis results obtained from RAPID were compared with results generated using a Representative Original Equipment Manufacturer (ROEM) method and a special purpose finite element program for fracture mechanics analysis and crack growth simulation in layered two dimensional structures. In general, results generated using RAPID were in good agreement with results generated using the ROEM method and the finite element code.

17. Key Words	18. Distribution Statement
Fastener Loads, Stress-Intensity Factors, Crack Growth, Residual Strength, Inspection Schedule	This document is available to the public through the National Technical Information Service (NTIS), Springfield, Virginia 22161.

19. Security Classif. (of this report)	20. Security Classif. (of this page)	21. No. of Pages	22. Price
Unclassified	Unclassified	29	

TABLE OF CONTENTS

LIST OF FIGURES

LIST OF SYMBOLS

a_{crit}	critical crack length
a_{det}	detectable crack length
a_i	initial crack length
a_f	final crack length
a_p	primary crack length
a_s	secondary crack length
A, B	fastener stiffness coefficients
C, p, q	Walker coefficients
D	fastener diameter
E	Young's Modulus
k_{fast}	fastener stiffness
K	stress-intensity factor
K_c	plane stress fracture toughness
N_{crit}	number of flights to reach critical crack length, a_{crit}
N_{det}	number of flights to reach a detectable crack length
N_{int}	inspection interval
N_{th}	inspection threshold
P	fuselage pressure differential
r	fuselage radius
R	minimum to maximum applied load ratio
S	applied tensile load
S_{res}	residual strength
t	thickness
W	width
β	boundary correction factor
ξ	ratio of bypass to gross stress
ζ	ratio of bearing to gross stress
$\sigma_{bearing}$	fastener bearing stress
σ_{bypass}	fastener bypass stress
σ_{gross}	fastener gross stress
σ_{lim}	limit load condition

EXECUTIVE SUMMARY

A critical issue identified by the aviation industry is the need to examine the effects of repairs on the structural integrity of aircraft. The incorporation of damage tolerance methodologies in the maintenance and repair practices of aging aircraft is required in order to insure their continued airworthiness and operational safety. In December 1978, the Federal Aviation Administration (FAA) amended their Fatigue Evaluation Requirements to include a damage tolerance philosophy. However, the majority of the current aircraft repairs are still designed using static strength approaches. The resources needed for damage tolerance designs of repairs are lacking, particularly for small operators and independent repair facilities. Consequently, inadequate repairs are being designed that do not meet damage tolerance requirements. In an effort to address this need, a task was undertaken to develop a new user-friendly software tool, Repair Assessment Procedure and Integrated Design (RAPID), capable of static strength and damage tolerance analyses of simple fuselage skin repairs.

A simplified engineering approach to static and damage tolerance analyses of riveted fuselage skin repairs has been incorporated in RAPID. In this study, the damage tolerance analysis methodology in RAPID was evaluated in terms of the fastener loads, stress-intensity factor solutions, crack growth, residual strength, and inspection schedule calculations. Three example problems, each representing a typical fuselage skin repair configuration, were analyzed. The analysis results obtained from RAPID were compared with results generated using a Representative Original Equipment Manufacturer (ROEM) method and a special purpose finite element program for fracture mechanics analysis and crack growth simulation in layered two-dimensional structures. In general, results generated using RAPID were in good agreement with results generated using the ROEM method and the finite element code.

INTRODUCTION

A critical issue identified by the aviation industry is the need to examine the effects of repairs on the structural integrity of aircraft. The incorporation of damage tolerance methodologies in the maintenance and repair practices of aging aircraft is required in order to insure their continued airworthiness and operational safety. In December 1978, the Federal Aviation Administration (FAA) amended their Fatigue Evaluation Requirements to include a damage tolerance philosophy. However, the majority of the current aircraft repairs are still designed using static strength approaches. The resources needed for damage tolerance designs of repairs are lacking, particularly for small operators and independent repair facilities. Consequently, inadequate repairs are being designed that do not meet damage tolerance requirements.

In an effort to address industries need for damage tolerance repair analysis capabilities, a task was undertaken to develop a new user-friendly software tool, Repair Assessment Procedure and Integrated Design (RAPID). The software tool conducts static strength and damage tolerance analyses of simple fuselage skin repairs and can be used to assess repair design and integrity, provide advice on repair design improvement, and provide data to establish an inspection program for the repair. The system is designed so that small independent repair stations and operators of small commuter airplanes will be able to use the tool.

RAPID is a simple, PC-based repair tool with a modularized open system architecture providing easy implementation of tool upgrades and new features. The current version of RAPID consists of five modules: Graphics User Interface (GUI), Advisory System (AS), Static Analysis (SA), Damage Tolerance Analysis (DTA), and Database modules. The GUI module is Windows™-based providing user-friendly, point-and-click, multitasking capabilities. The AS module provides generic engineering guidelines for specifying fastener arrangements, doubler materials, and doubler thicknesses. The SA module performs static strength analysis of repair configurations based on the fastener shear allowables, skin hole bearing allowables, and doubler tensile allowables. The DTA module calculates the critical fastener loads and applies a simplified crack growth algorithm to determine crack growth and residual strength and provides an inspection schedule. The Database module consists of material database containing elastic, strength, crack growth, fracture properties, and a fastener database containing fastener shear allowables and skin hole bearing allowables.

In this study, the damage tolerance analysis methodology in RAPID was evaluated in terms of the fastener loads, stress-intensity factors, crack growth, residual strength, and inspection schedule. Three example problems, each representing a typical fuselage skin repair configuration, were analyzed. The analysis results obtained from RAPID were compared with results generated using a Representative Original Equipment Manufacturer (ROEM) approach and the Fracture Analysis Code for 2-Dimensional Layered (FRANC2DL) structures, a special purpose finite element program for fracture mechanics analysis and crack growth simulation in layered two-dimensional structures.

In the following sections, the damage tolerance methodology is highlighted and the models used in the FRANC2DL and the ROEM analysis are presented. The results are then compared in terms of the fastener loads, stress-intensity factor solutions, crack growth characteristics, residual strength, and inspection schedules.

APPROACH

RAPID DAMAGE TOLERANCE METHODOLOGY.

The damage tolerance analysis in RAPID is based on the approach outlined by Swift [1]. The procedure involves several steps including the calculation of fastener loads, assumption of the initial flaw geometry and growth, and calculations of stress-intensity factor, crack growth, residual strength, and inspection schedule. Each of these components is discussed in the following paragraphs.

FASTENER LOADS. A single-strip model is used to determine the stresses in the vicinity of the critical fastener hole. In the analysis, the skin bypass stress σ_{bypass} and skin bearing stress $\sigma_{bearing}$ at the critical fastener hole are calculated due to the applied tensile gross stress σ_{gross}. The skin and doubler are idealized as axial rods having stiffnesses equal to AE/L where A is the cross section area, E is the modulus, and L is axial length. The fastener stiffness is expressed empirically as [1]:

$$k_{fast} = \frac{E'D}{A + B\left(\frac{D}{t_s} + \frac{D}{t_d}\right)} \tag{1}$$

where A and B are curve fitting parameters, E' is the effective modulus of the skin and doublers, t_s and t_d are the skin and doubler thicknesses, and D is the fastener diameter. For aluminum fasteners, A = 5.0 and B = 0.8. Using a standard matrix method of structural analysis, the skin internal loads, σ_{bypass} and $\sigma_{bearing}$, can be determined and expressed in terms of σ_{gross}:

$$\sigma_{bypass} = \xi\sigma_{gross}\ , \qquad \sigma_{bearing} = \zeta\sigma_{gross} \tag{2}$$

where ξ is the ratio of bypass to gross stress, and ζ is the ratio of bearing to gross stress.

INITIAL FLAW GEOMETRY AND GROWTH. An initial flaw geometry is assumed. The two initial crack cases available in RAPID are shown in figure 1. For the first case, the initial flaw consists of a primary crack, a_p = 0.05", and a secondary crack, a_s = 0.005", at the edge of the center fastener hole. For the second case, the initial flaw consists of a single crack, a_p = 0.05", at the edge of the center fastener hole. The subsequent crack growth scenarios are also illustrated in figure 1. For the first case, when the primary crack grows into the first adjacent hole, a crack of length 0.005" is then assumed to initiate on the opposite side. For the second case, when the primary crack grows into the adjacent hole, cracks of length 0.005" are assumed on the opposite side of each of the two holes. Whenever a crack enters a hole, a crack of length 0.005" is assumed to initiate on the opposite side of the hole.

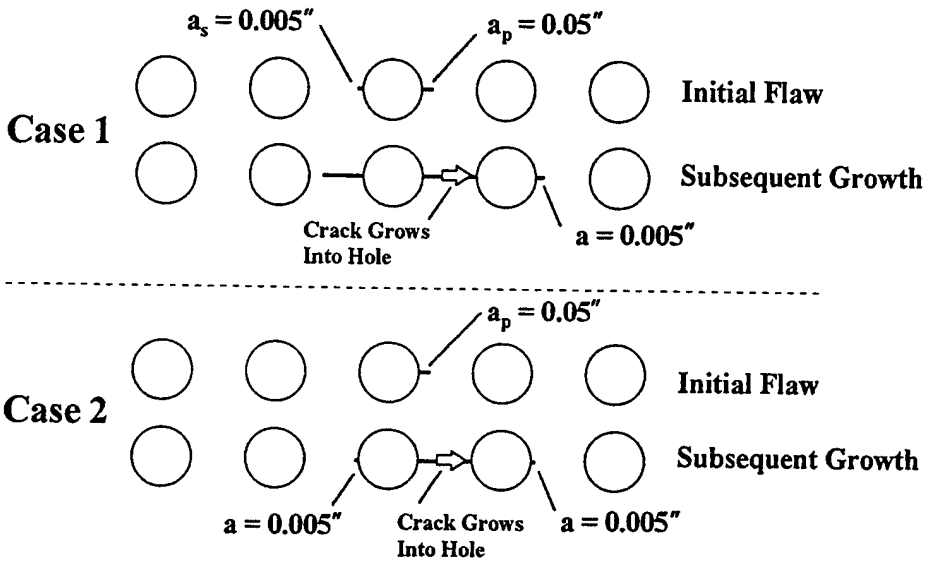

FIGURE 1. THREE INITIAL FLAW GEOMETRIES AND SUBSEQUENT GROWTH

STRESS-INTENSITY FACTOR. There are five baseline stress-intensity factor (SIF) solutions in RAPID as shown in figure 2: (1) a single crack emanating from a hole in an infinite plate subjected to far-field tension; (2) a single crack emanating from a hole in an infinite plate subjected to a pair of pin loads; (3) two cracks of unequal length emanating from a hole in an infinite plate subjected to far-field tension; (4) two cracks of unequal length emanating from a hole in an infinite plate subjected to a pair of pin loads; and (5) a crack in an infinite plate approaching an open hole subjected to far-field tension. Methods of superposition, compounding, and similarity are used to determine the SIF needed during the simulation of crack growth. The SIF is expressed in terms of the applied stress, S, crack length, a, and a boundary correction factor, β, as $K = S\beta\sqrt{\pi a}$

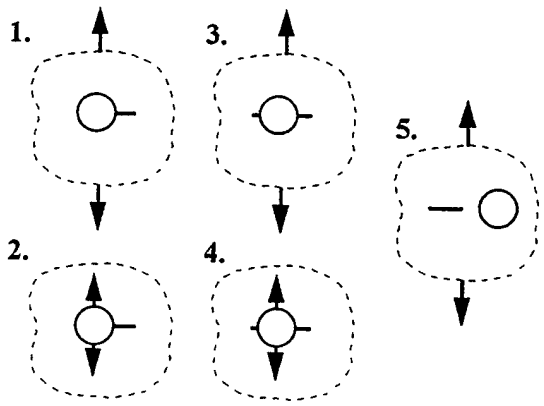

FIGURE 2. FIVE BASELINE STRESS-INTENSITY FACTOR SOLUTIONS IN RAPID

CRACK GROWTH MODEL. A simplified crack growth model based on Walker's equation is used:

$$\frac{da}{dN} = C\left\{(1-R)^q K_{max}\right\}^p \tag{3}$$

where R is the stress ratio, K_{max} is the maximum stress-intensity factor (due to σ_{bypass}, $\sigma_{bearing}$, and σ_{gross}), and C, p, and q are material coefficients. Inverting and integrating equation 3 and separating geometry, load, and material terms yields an expression for the number of cycles:

$$N = \frac{1}{C}\left\{\frac{1}{S(1-R)^q}\right\}^p \int_{a_i}^{a_f} \frac{da}{\left(\beta\sqrt{\pi a}\right)^p} \tag{4}$$

The first terms in front of the integral are the load and material terms where S is the maximum applied stress. In this study, a constant amplitude stress is assumed where $R = 0$ and $S = \sigma_{gross}$. The integral is the geometry term where a_i is the initial crack length, a_f is the final crack length, and β is the boundary correction factor. Gauss numerical integration is used to solve equation 4.

RESIDUAL STRENGTH. The residual strength S_{res} is then calculated in terms of the skin plane stress fracture toughness K_c, the crack length a, and the boundary correction factor, β:

$$S_{res} = \frac{K_c}{\beta\sqrt{\pi a}} \tag{5}$$

INSPECTION THRESHOLD AND INTERVAL. The inspection threshold is calculated in RAPID from

$$N_{th} = \frac{N_{crit}}{2} \tag{6}$$

where N_{crit} is the number of flights for the crack to propagate from an initial flaw size of 0.05" to the critical size, a_{crit}, under the limit load condition. The limit load condition was derived from the damage tolerance evaluation requirements specified in FAR §25.571 and is assumed to be the following:

$$\sigma_{lim} = \frac{1.1(P+0.5)r}{t} \tag{7}$$

where P is the pressure differential of the fuselage, r is the fuselage radius, and t is the fuselage skin thickness. The critical crack length is given in terms of the limit load condition and plane stress fracture toughness:

$$a_{crit} = \frac{{K_c}^2}{\left(\sigma_{lim}\beta\right)^2 \pi} \tag{8}$$

The inspection interval is calculated in RAPID by the following equation:

$$N_{int} = \frac{N_{crit} - N_{det}}{2} \tag{9}$$

where N_{det} is the number of flights to reach a crack size that is detectable for a specific nondestructive inspection (NDI) method of crack detection.

FRANC2DL MODELS.

The Fracture Analysis Code for 2-Dimensional Layered (FRANC2DL) structures is a special purpose finite element program with fracture mechanics analysis and crack growth simulation capabilities [2]. FRANC2DL was used to evaluate the fastener loads, stress-intensity factors, crack growth, and residual strength for a repair consisting of a single doubler mechanically fastened to the skin using a single fastener type. The initial flaw geometry and assumed growth scenario were chosen to be identical to Case 2 shown in figure 1. A description of the models used in FRANC2DL are provided below.

FASTENER LOAD MODELS. A single-strip model consisting of two 1-in-wide strips (one skin strip and one doubler strip) mechanically fastened using a single row of rivets with a 1-in pitch was used to calculate the fastener loads. Two cases were used: (1) a strip model fastened with five rivets with both the skin and doubler strips fixed on one end, and a 1-ksi stress applied to the skin on the other end, and (2) a strip model fastened with three rivets with the doubler strip fixed on one end and a 1-ksi stress applied to the skin on the other end. For both cases, the skin and doubler had the same thickness, $t_s = t_d = 0.04$", and the same mechanical properties: Young's modules $E_s = E_d = 10.5$E06 psi, and Poisson's ratio $\nu_s = \nu_d = 0.33$. Aluminum rivets were assumed with a diameter $D = 0.1875$". Using equation 1 the fastener stiffness was calculated as $k_{fast} = 157500$ lb/in.

STRESS-INTENSITY FACTOR. To illustrate the computation of the SIF, the repair configuration shown in figure 3 was used.

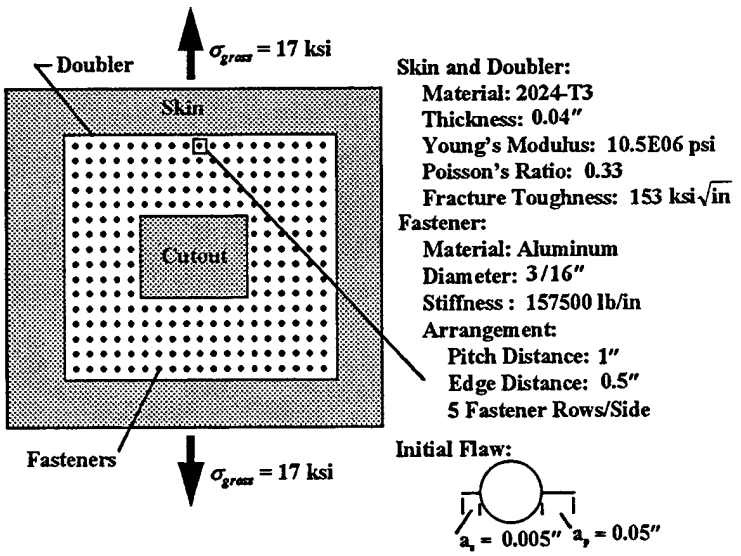

FIGURE 3. DESCRIPTION OF REPAIR CONFIGURATION

The skin and doubler had the same thickness, $t_s = t_d = 0.04$", and the same mechanical properties: Young's modulus $E_s = E_d = 10.5$E06 psi, Poisson's ratio $\nu_s = \nu_d = 0.33$, and fracture toughness $K_c^s = K_c^d = 153$ ksi-in$^{1/2}$. The rivets were aluminum with a diameter $D = 0.1875$" and a stiffness

k_{fast} = 157,500 lb/in calculated from equation 1. The fastener arrangement consists of five rivet rows per repair side with a pitch distance of 1" and an edge distance of 0.5". An initial flaw was assumed at the edge of the middle hole in the first fastener row consisting of a primary crack of length a_p = 0.05" and a secondary crack of length a_s = 0.005". A remote tensile stress of σ_{gross} = 17 ksi was applied to the skin.

Two idealizations shown in figure 4 were used to represent the repair configuration shown in figure 3. First, a single-strip model was used to determine the bearing stress, $\sigma_{bearing}$, and bypass stress, σ_{bypass} , at the critical fastener hole. Then a plate (skin) model containing a periodic array of holes was used to determine the SIF due to the applied, bearing, and bypass stresses. For the loading on the single-strip model, the results from RAPID were used where σ_{gross} = 17 ksi, $\sigma_{bearing}$ = 27.0667 ksi, and σ_{bypass} = 11.92 ksi. These stresses were then applied to the plate model and the SIF was calculated at various crack lengths up to the second breakthrough condition. Breakthrough is defined as the condition where the crack grows into the next hole. Symmetric loading conditions were applied to the plate model using the method of superposition.

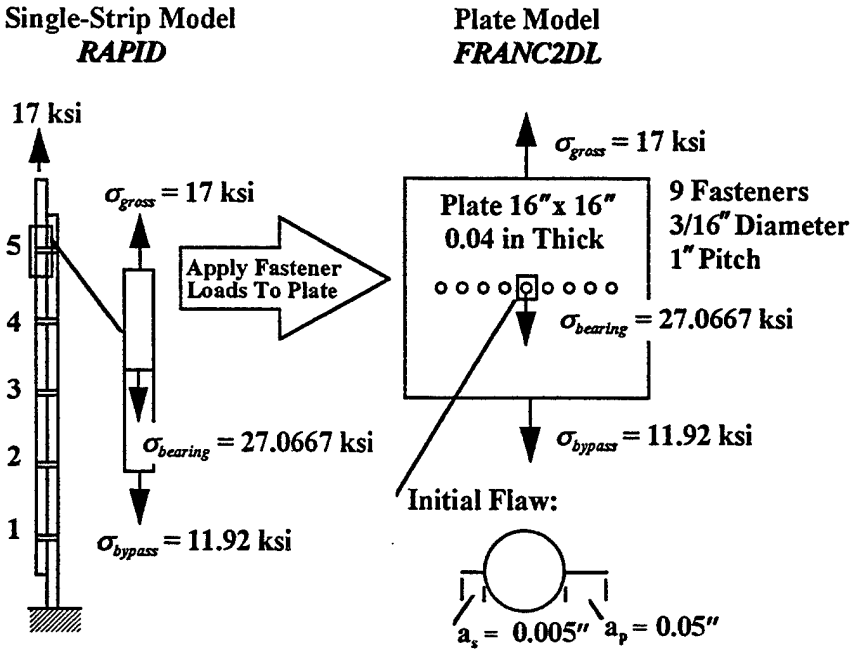

FIGURE 4. MODELS USED TO REPRESENT REPAIR CONFIGURATION

Three cases with various loading and fastener arrangements were analyzed for the plate model as shown in figure 5. For Case 1, a plate containing nine fastener holes was subjected to a remote stress of 1/2(σ_{gross} + σ_{bypass}) and a pair of bearing loads 1/2($\sigma_{bearing}$) at all fastener holes. For Case 2, a plate containing nine fastener holes was subjected to two loading conditions: (1) from the initial flaw to the first breakthrough, a remote tensile stress of 1/2(σ_{gross} + σ_{bypass}) was applied in the far-field and a pair of bearing loads 1/2($\sigma_{bearing}$) was applied to the middle fastener hole

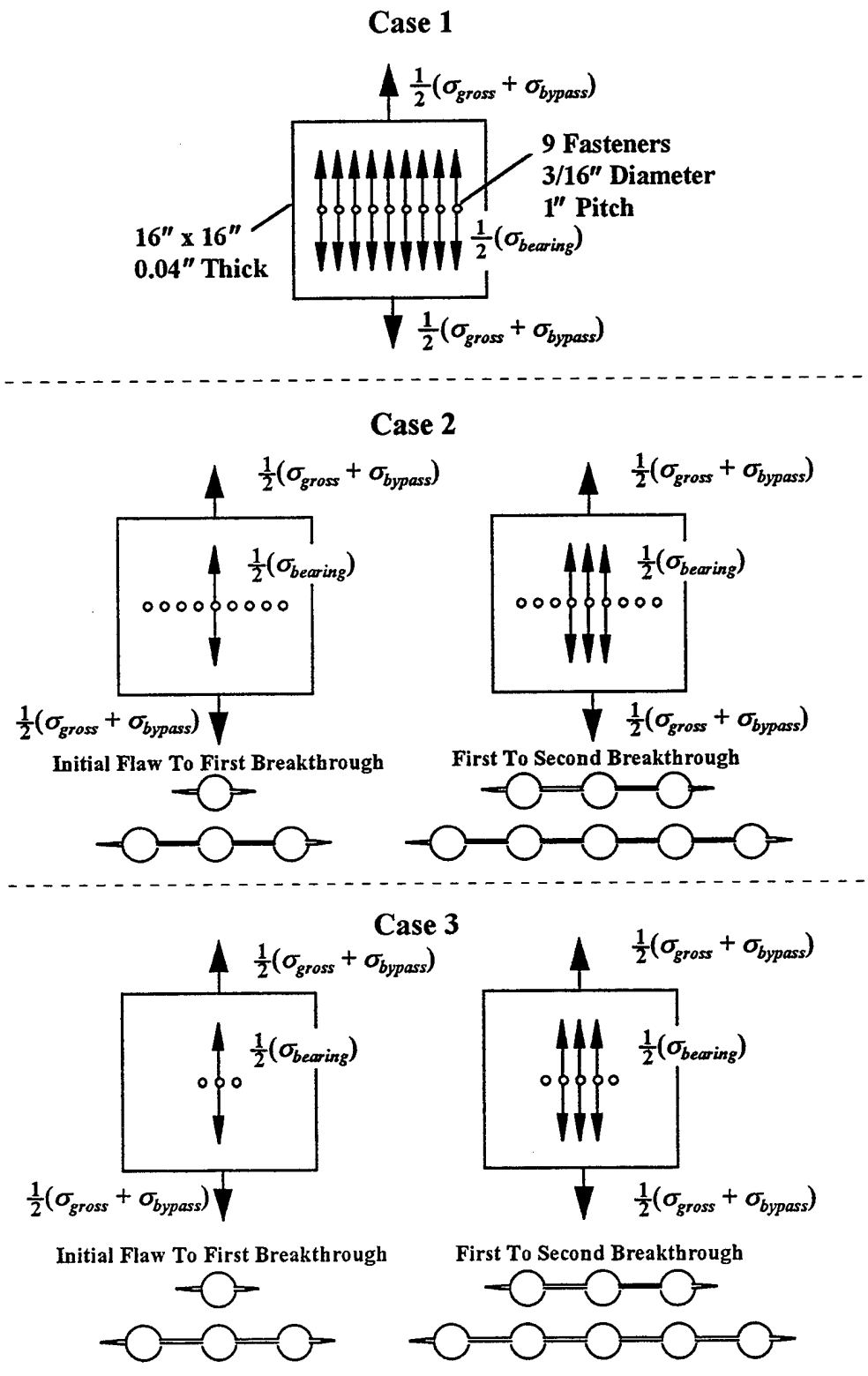

FIGURE 5. APPLIED LOADING AND FASTENER ARRANGEMENT FOR THE FRANC2DL MODELS

containing the initial flaw, and (2) from the first breakthrough to the second breakthrough, a remote tensile stress of $1/2(\sigma_{gross} + \sigma_{bypass})$ was applied in the far-field and a pair of bearing loads $1/2(\sigma_{bearing})$ was applied to the middle three fastener holes which were connected by cracks. For Case 3 two different fastener and loading arrangements were considered: (1) from the initial flaw to the first breakthrough, a plate containing three fastener holes was subjected to a remote tensile stress of $1/2(\sigma_{gross} + \sigma_{bypass})$ and a pair of bearing loads $1/2(\sigma_{bearing})$ at the middle fastener hole containing the initial flaw, and (2) from the first breakthrough to the second breakthrough, a plate containing five fastener holes was subjected to remote tensile stress of $1/2(\sigma_{gross} + \sigma_{bypass})$ and a pair of bearing loads $1/2(\sigma_{bearing})$ at the middle three fastener holes which were connected by cracks. Of these three cases, Case 3 most closely resembles the loading and fastener arrangement conditions used in the RAPID damage tolerance analysis described earlier.

Figure 6 shows the two finite element meshes which were used to analyze the three cases studied. The first mesh was used for crack lengths between the initial flaw up to the first breakthrough condition. This mesh consisted of 3008 eight-noded elements. The second mesh was used for crack lengths from the first breakthrough up to the second breakthrough condition. This mesh consisted of 3172 eight-noded elements. Both meshes changed automatically during the analysis due to the adaptive meshing used in FRANC2DL when cracks are introduced.

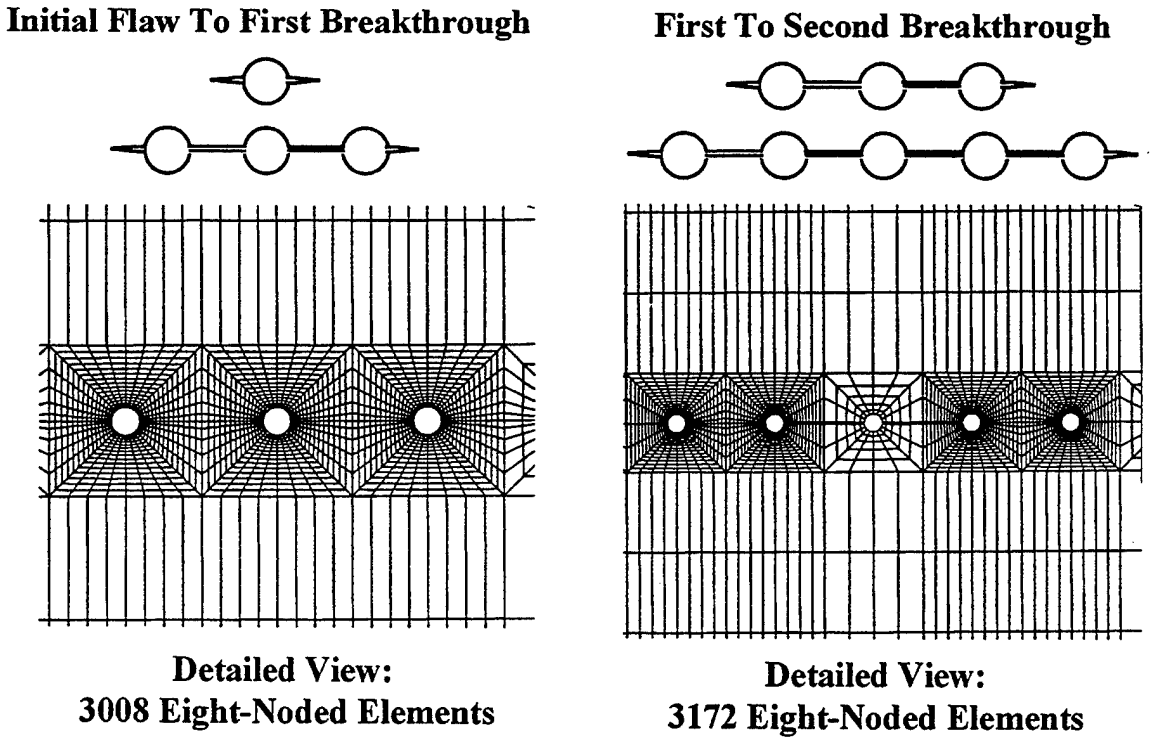

FIGURE 6. FINITE ELEMENT MESHES USED IN THE FRANC2DL ANALYSIS

CRACK GROWTH AND RESIDUAL STRENGTH. Eight steps were used to calculate the crack growth and residual strength:

1. Assume an initial flaw size for the primary and secondary crack lengths, a_p and a_s.
2. Extend the primary crack, $\Delta a_p = 0.1 a_p$.
3. Calculate the stress-intensity factors (SIF) for both the primary and secondary cracks K_p^{max} and K_s^{max}.
4. Calculate the crack growth rate of the primary crack, da_p/dN, using Walker's equation.
5. Calculate the cycle interval corresponding to the primary crack extension, $\Delta N = (dN/da_p)\Delta a_p$.
6. Extend the secondary crack over the cycle interval, $\Delta a_s = (da_s/dN)\Delta N$.
7. Sum the crack lengths for the primary and secondary cracks, $a = a + \Delta a$.
8. Calculate the residual strength for the primary and secondary cracks, $S_{res} = \sigma_{gross} K_c / K^{max}$.

Steps 2 through 8 are repeated until the second breakthrough occurs.

REPRESENTATIVE ORIGINAL EQUIPMENT MANUFACTURER (ROEM) APPROACH.

Results from the damage tolerance analysis methodology in RAPID were also compared to results generated using a Representative Original Equipment Manufacturer (ROEM) approach. In the ROEM approach, the method used to determine the critical fastener location and the fastener load is the same as that used in RAPID. However, the initial flaw crack geometry and the crack growth simulation procedure differ from those in RAPID shown in figure 1. It is assumed in the ROEM approach that a primary and a secondary cracks of sizes 0.05" and 0.005", respectively, exists at both sides of the critical fastener hole. In addition, it is assumed that secondary cracks of size 0.005" exists on both sides of the remaining fastener holes. The growth of each crack is assumed to occur simultaneously but independently. That is, the interaction between the crack tips is ignored in the stress-intensity factor solutions for the individual cracks.

In the ROEM approach, three examples representing typical fuselage skin repair configurations were analyzed. Repair type I consists of a single external doubler mechanically fastened over a cutout using two types of fasteners as shown in figure 7. Repair type II consists of an internal and external doubler mechanically fastened using three fastener types as shown in figure 8. Repair type III consists of a skin cutout and two external doublers mechanically fastened using three fastener types as shown in figure 9. The crack growth and inspection schedule were calculated using RAPID and the ROEM approach.

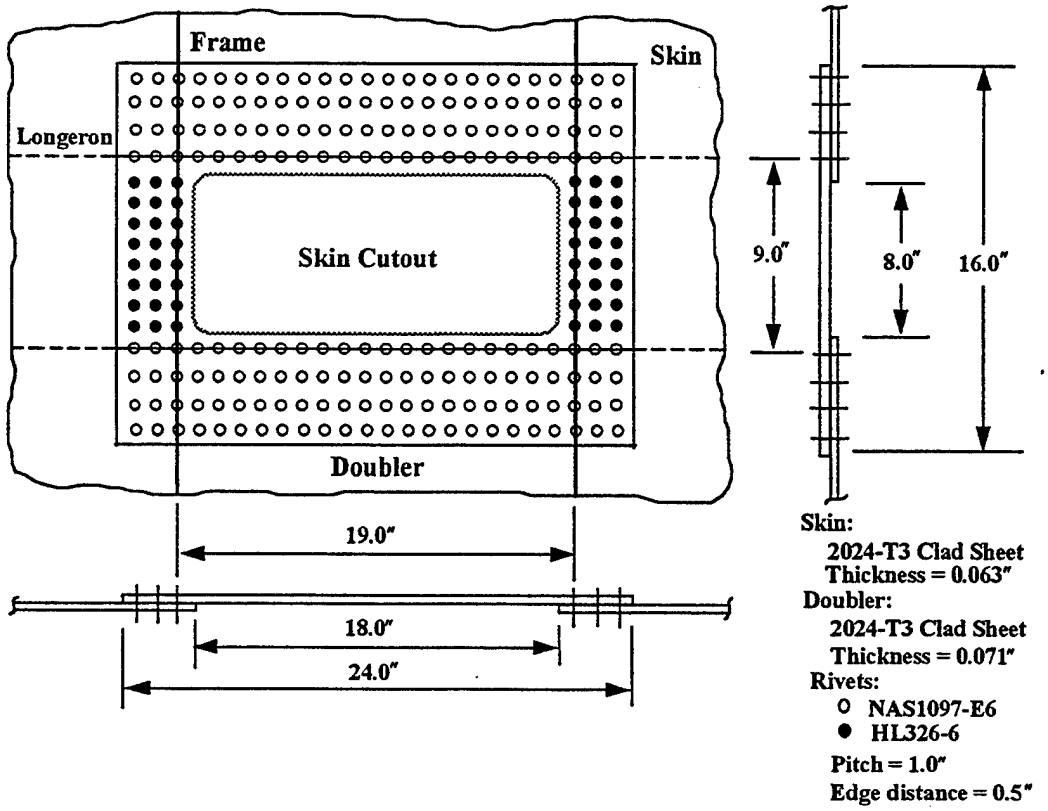

FIGURE 7. DEFINITION OF REPAIR TYPE I USED IN ROEM ANALYSIS

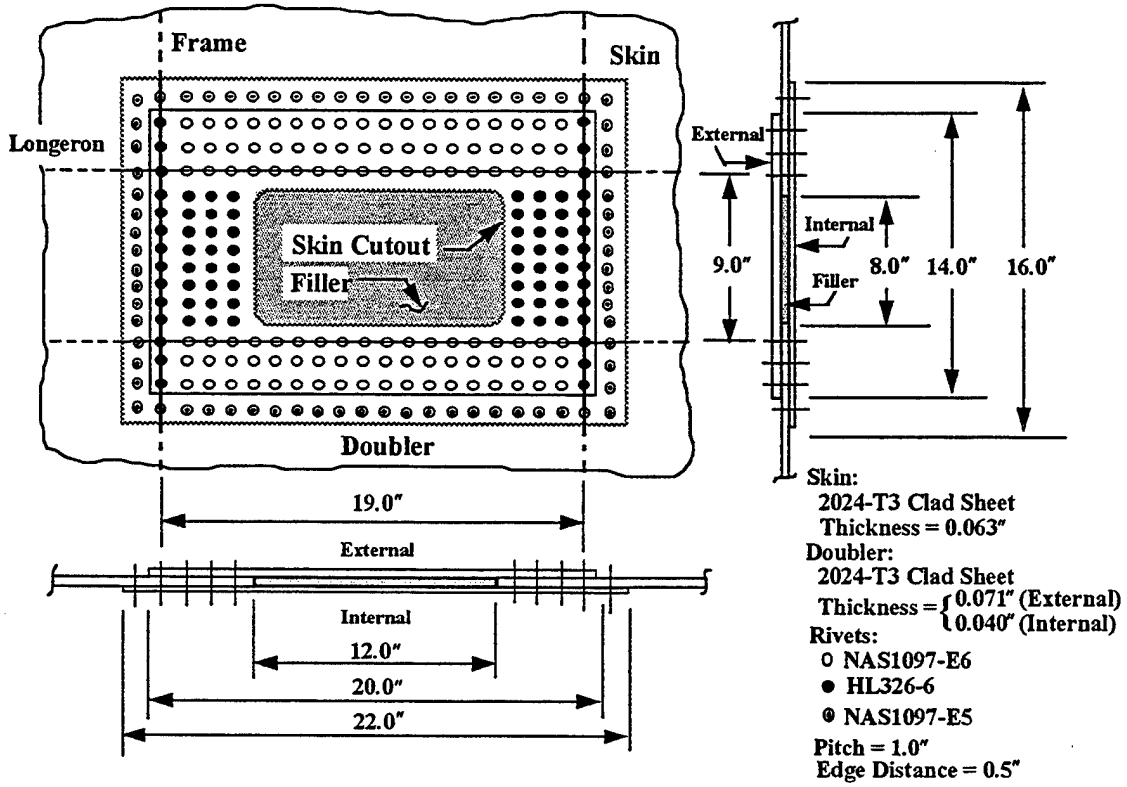

FIGURE 8. DEFINITION OF REPAIR TYPE II USED IN ROEM ANALYSIS

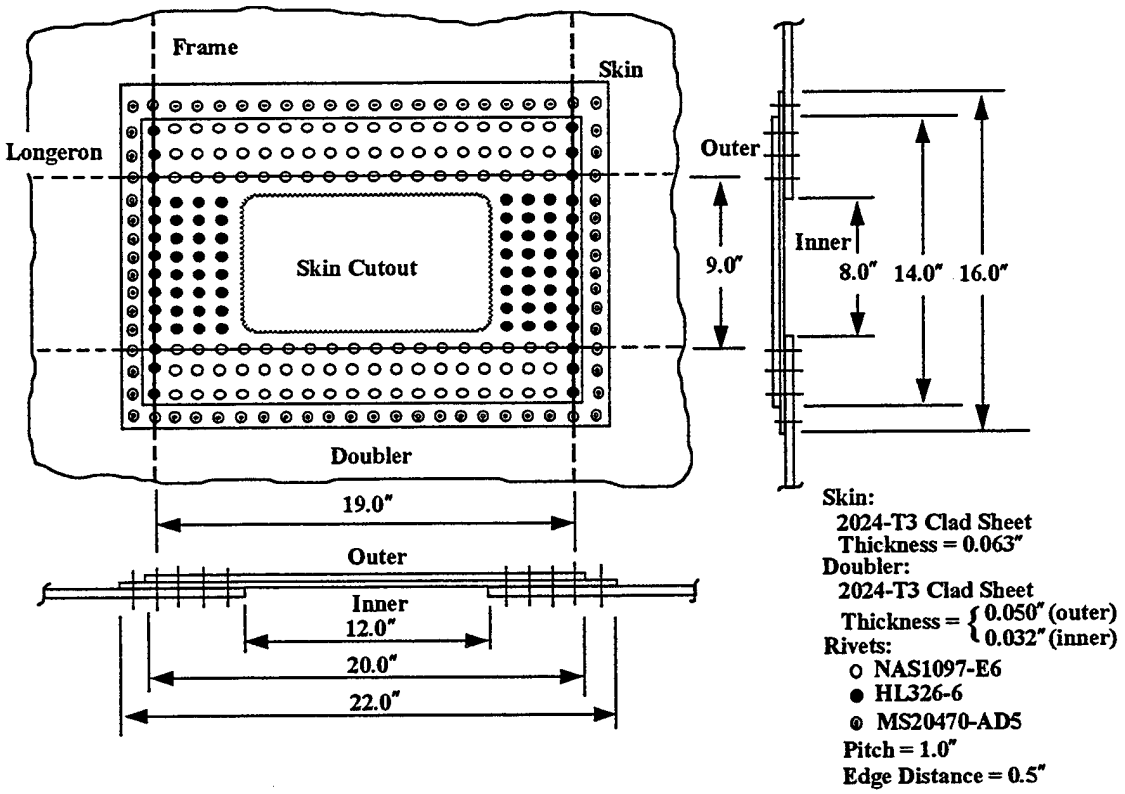

FIGURE 9. DEFINITION OF REPAIR TYPE III USED IN ROEM ANALYSIS

RESULTS AND DISCUSSION

FASTENER LOADS.

A comparison of the calculated fastener loads using RAPID and FRANC2DL is shown in figure 10. As shown in the figure, the model consists of a skin and doubler strips fastened using three fasteners. On one end, the doubler is held fixed, and on the other end, a unit stress is applied to the skin. These boundary conditions model the skin cutout. As indicated in this figure, the critical fastener with the highest load calculated using FRANC2DL was approximately 1 percent lower then that calculated using RAPID.

In another comparison of the fastener load calculations, a different model was considered as shown in figure 11. As shown in the figure, the model consists of a skin and doubler strips fastened using five fasteners. On one end, both the skin and doubler are held fixed, and on the other end, a unit stress is applied to the skin. In this figure, results published by Swift [1] was used as a baseline solution to ensure that the finite element model used in the FRANC2DL analysis yielded sensible results. As indicated in the figure, the fastener loads calculated using FRANC2DL were in good agreement with results published by Swift [1]. For the critical fastener with the highest load, the difference in the results was less than 1 percent, figure 11.

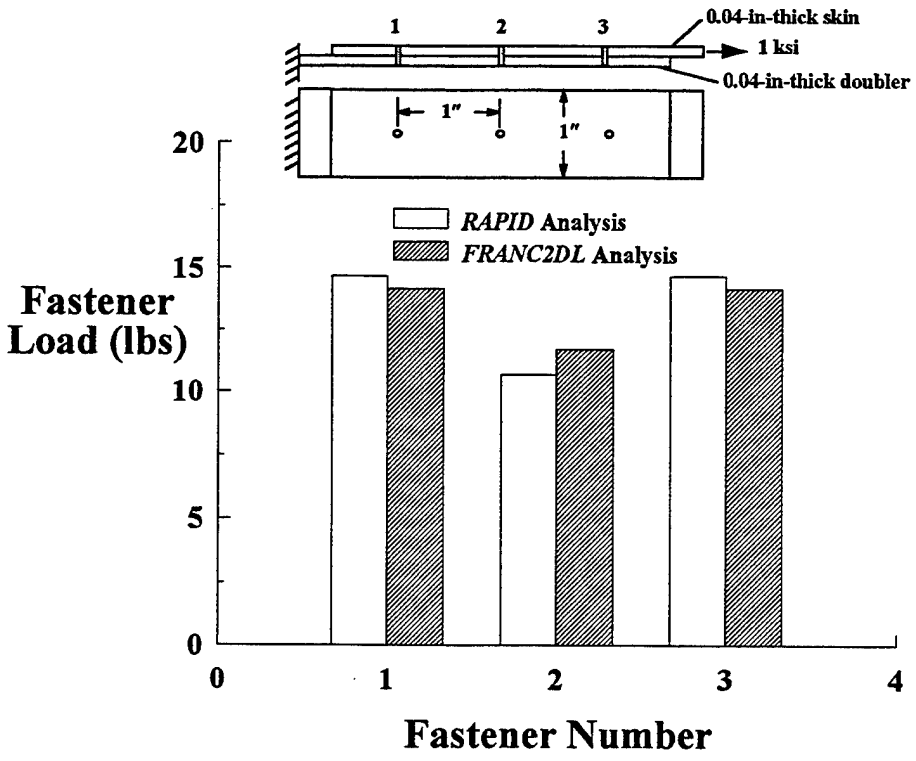

FIGURE 10. CALCULATED FASTENER LOADS FROM RAPID AND FRANC2DL

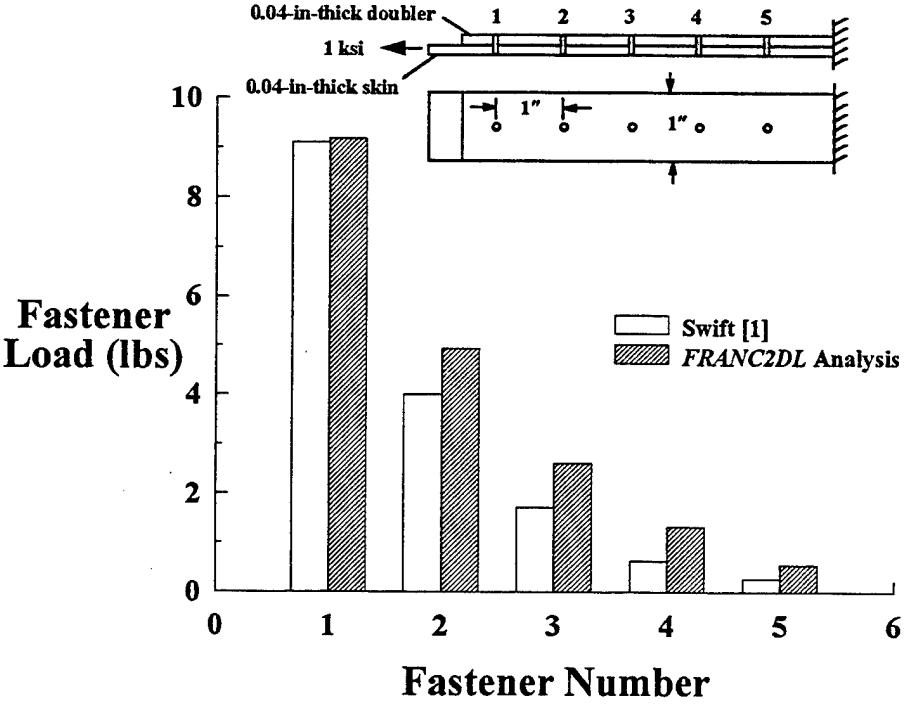

FIGURE 11. FASTENER LOADS CALCULATED USING FRANC2DL AND RESULTS FROM REFERENCE 1

STRESS-INTENSITY FACTOR SOLUTIONS.

Using FRANC2DL, the SIF as a function of crack length for the primary crack was calculated for all three cases and compared with RAPID calculations as shown in figure 12. In general, the SIF solutions calculated for Case 1 were the largest values while the solutions calculated using RAPID were the lowest values. Results for Cases 2 and 3 were in the middle. The trends for all results were the same; the SIF values increased with crack length. As the crack tip approached the first hole, the SIF values increased substantially. The local net section stresses increase as the crack tip approaches the hole. The concentration of stress along the hole boundary causes the SIF to increase. A step-wise decrease in the value of the SIF occurred immediately after the first breakthrough. Lower stresses in the net section ligament length between the crack tip and the second fastener hole caused a decrease in the value of the SIF. The SIF values then increased with increase in crack length. The rate of increase of the SIF decreased as the crack length increased. As the crack approached the second hole, the rate of increase of the SIF again increased due to the hole boundary effect.

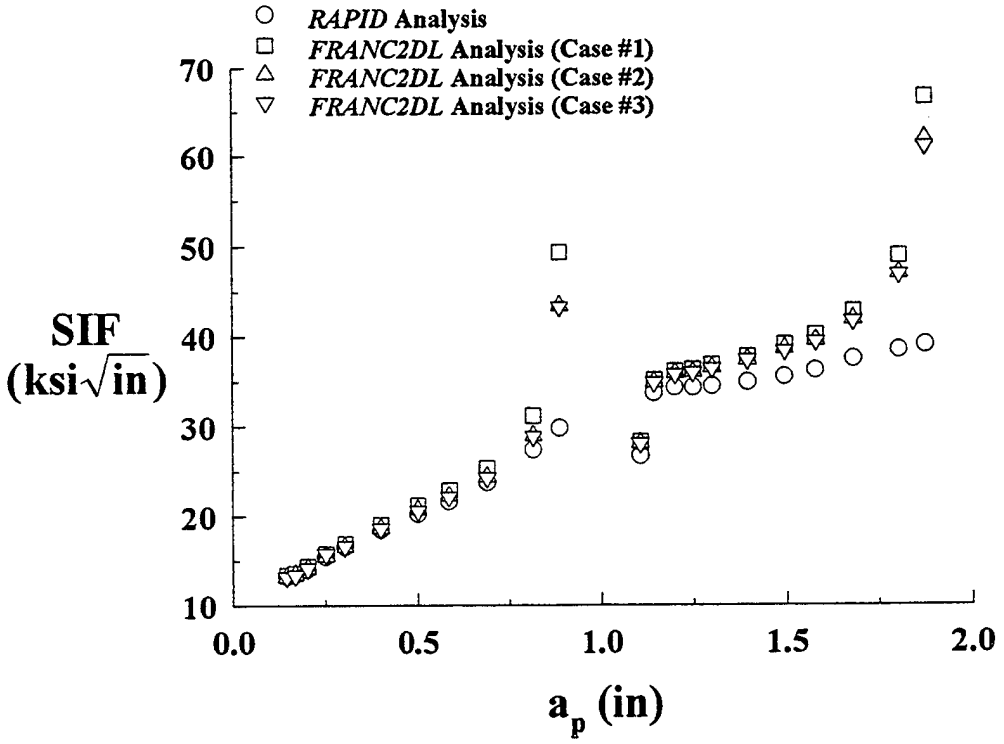

FIGURE 12. STRESS-INTENSITY FACTOR AS A FUNCTION OF CRACK LENGTH

For crack growth within two hole diameters of the initial crack, there was good agreement between the RAPID results and all three FRANC2DL results, with a maximum difference of 2 percent. Modeling the loaded hole in front of the crack tip only marginally increased the SIF solution. As the crack length increased and approached the first hole, the difference in values increased substantially. Here the effect of modeling a loaded hole in front of the crack tip can be seen by comparing results from Case 1 with the other results. The SIF results for Case 1 were

substantially higher. In addition, modeling an array of holes in front of the crack tip did not affect the SIF results as seen by comparing results of Cases 2 and 3. Thus, modeling an array of holes in front of the crack tip is not necessary. The RAPID approximation does not fully capture the singularity as the crack tip approaches the hole, however, this occurs over a very short crack extension length.

After the first breakthrough condition, there was a maximum of a 5 percent difference in the solutions for crack lengths up to approximately 25 percent of the ligament length between the first and second breakthrough holes. From this point forward, the difference increased as the crack length increased. Contributing to this increased difference is the effect due to the finite width of the finite element models (RAPID assumes crack growth in an infinite body). For crack lengths over 50 percent of the ligament length between the first and second breakthrough holes, the tip-to-tip a/W ratio was approximately 0.2. For this a/W ratio, it is expected that the SIF calculated using FRANC2DL would be 5 percent higher than the RAPID results due to the finite width effect.

CRACK GROWTH.

The length of the primary crack as a function of the number of flights was calculated using FRANC2DL and compared with RAPID results as shown in figure 13. In this figure, the primary crack length, a_p, is measured from the tip of the crack to the centerline of the initial hole. In general, the results are in good agreement. Differences in the crack growth predictions are due mainly to the differences in the SIF calculations as discussed previously. For crack lengths up to approximately 50 percent of the first breakthrough condition, the corresponding number of flights

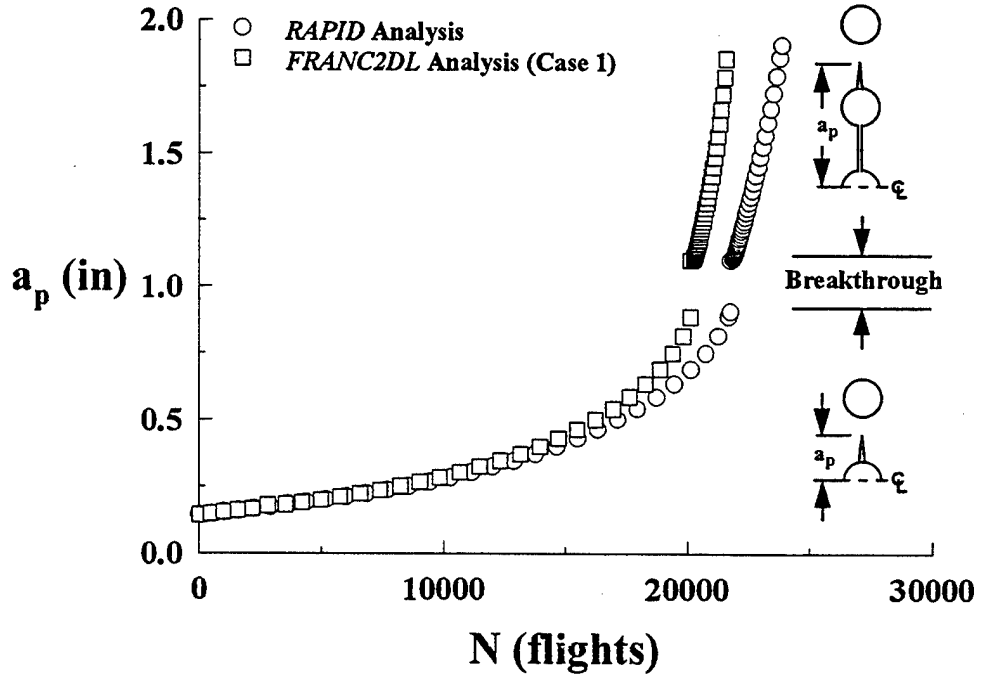

FIGURE 13. CRACK LENGTH AS A FUNCTION OF THE NUMBER OF FLIGHTS

calculated using RAPID was 5 percent higher than the FRANC2DL results. As the crack length increased and approached the first hole, the number of flights calculated using RAPID was approximately 8 percent higher than the FRANC2DL result. Up to the second breakthrough, the number of flights calculated using RAPID was 10 percent higher than the FRANC2DL result. Better agreement would be obtained using Cases 2 and 3 which better resemble the loading conditions used in RAPID.

The crack length as a function of the number of flights was calculated using the ROEM approach for the three repair types and compared with results generated using RAPID as shown in figures 14-16. In general, a slow crack growth process was predicted up to the first breakthrough condition for both analysis. At the first breakthrough condition, the ROEM analysis predicts sudden catastrophic fracture of the repair skin. The RAPID analysis predicts a more stable crack growth process where at least two breakthrough conditions occurred prior to catastrophic fracture of the repair skin. The difference in the results using the two methods is due to the differences in the initial flaw assumptions. In the ROEM approach, primary and secondary cracks of lengths 0.05" and 0.005", respectively, exists at both sides of the critical fastener hole and secondary cracks of length 0.005" exists on both sides of the remaining fastener holes. The growth of each crack is assumed to occur simultaneously but independently. In the RAPID analysis, the Case 2 crack growth scenario shown in figure 1 was assumed.

The crack growth results for repair type I are shown in figure 14. For the ROEM analysis, the first breakthrough condition occurred at 47,000 flights, where the initial primary crack grew to the

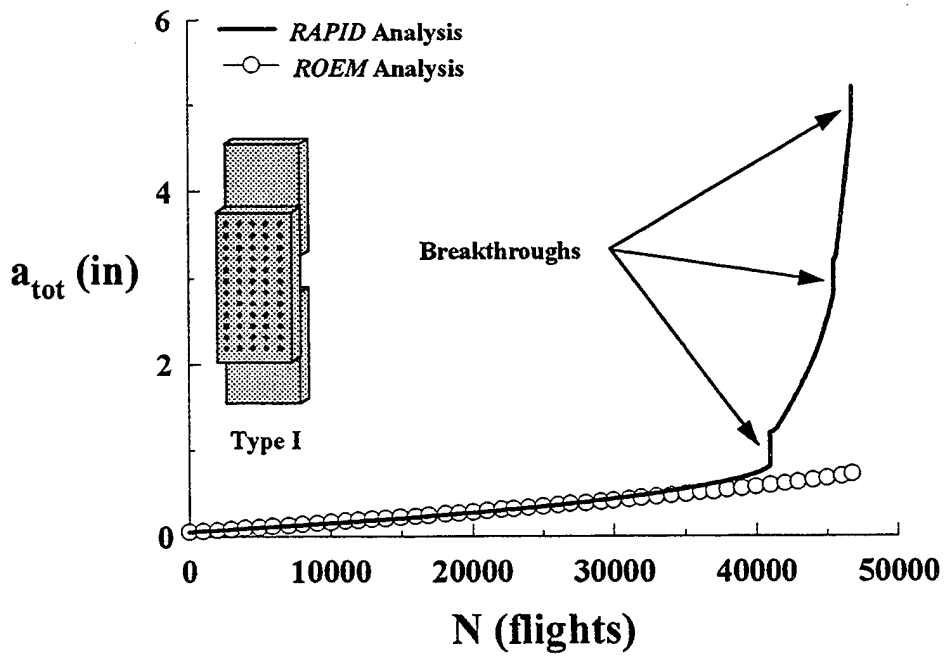

FIGURE 14. TOTAL CRACK LENGTH AS A FUNCTION OF THE NUMBER OF FLIGHTS FOR TYPE I REPAIR

adjacent hole and the initial secondary cracks grew independently to lengths of 0.525". At these crack growth lengths, all cracks linked up to form a single crack resulting in sudden catastrophic fracture of the repair skin. For the RAPID analysis shown in figure 14, the first breakthrough occurred at 41,000 flights where the initial primary crack grew to the adjacent hole. Secondary cracks then initiated at opposite sides of the holes as shown schematically for Case 2 in figure 1. The subsequent crack growth rate increased with the second breakthrough occurring at 45,515 flights. The RAPID analysis indicated that catastrophic fracture of the repair skin occurred after the third breakthrough at 46,805 flights.

Trends for the results for repair types II and III shown in figures 15 and 16, respectively, are similar to those in figure 14. For the ROEM analysis, the first breakthrough condition for repair type II and III occurred at 53,100 and 53,586 flights, as shown in figures 15 and 16. After the first breakthrough condition, sudden catastrophic fracture of the repaired skin was predicted using the ROEM analysis. For the RAPID analysis, the first breakthrough condition for repair type II and III occurred at 48,416 and 48,928 flights, as shown in figures 15 and 16. Fracture of the repaired skin after the second breakthrough condition was predicted using the RAPID analysis at 53,100 and 53,586 flights for repair types II and III, respectively.

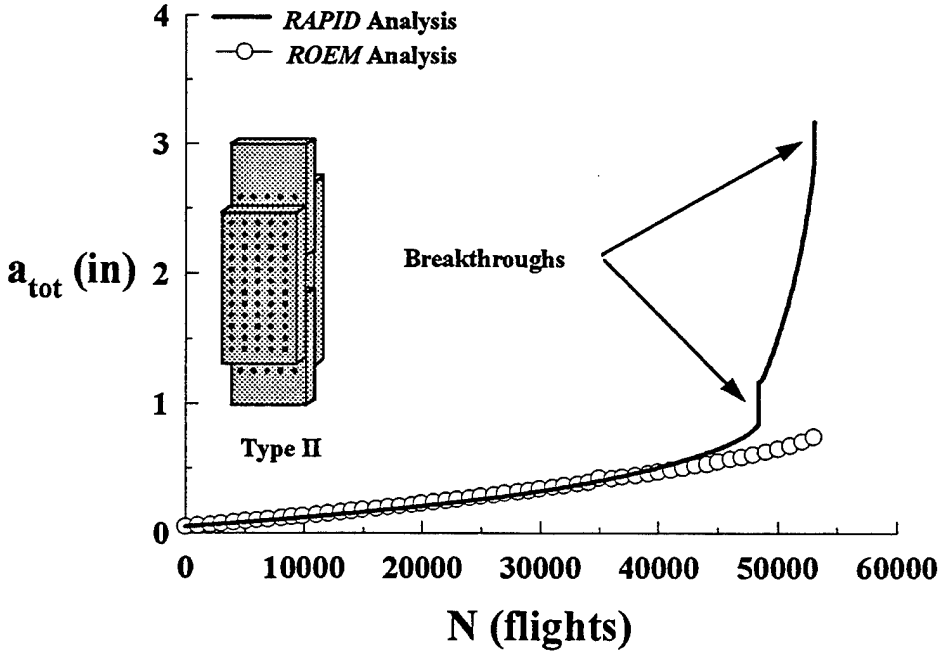

FIGURE 15. TOTAL CRACK LENGTH AS A FUNCTION OF THE NUMBER OF FLIGHTS FOR TYPE II REPAIR

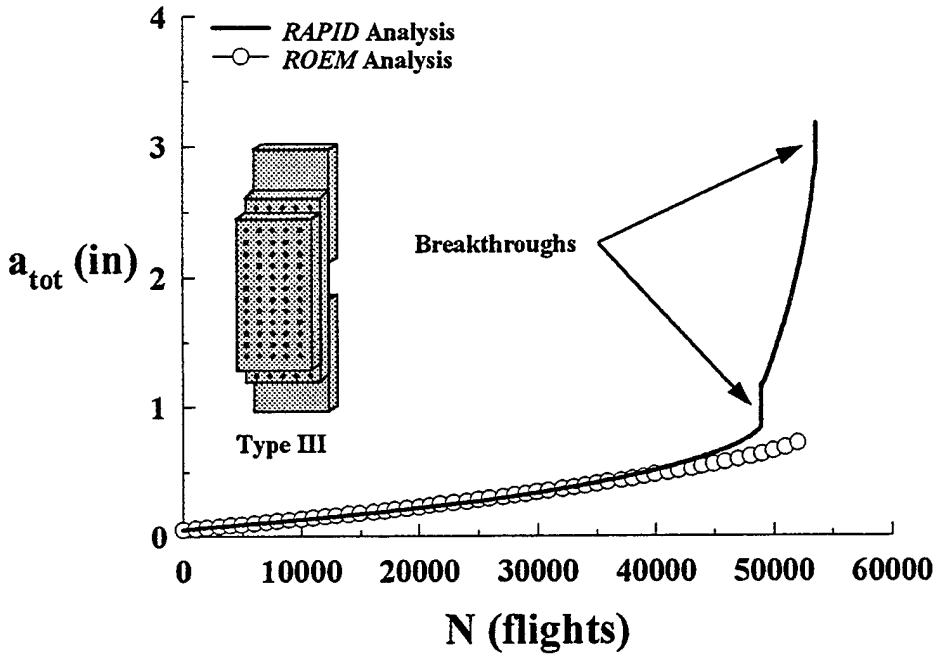

FIGURE 16. TOTAL CRACK LENGTH AS A FUNCTION OF THE NUMBER OF FLIGHTS FOR TYPE III REPAIR

RESIDUAL STRENGTH.

Residual strength as a function of crack length for the primary crack was calculated using RAPID and FRANC2DL as shown in figure 17. The residual strength, S_{res}, was calculated using equation 5. Case 1 shown in figure 5 was used in the FRANC2DL analysis. In general, the trends for the results were the same; the residual strength values decreased with crack length. As the crack tip approached the first hole, the residual strength values decreased substantially due to hole boundary effects. The residual strength is inversely proportional to the SIF term (denominator) in equation 5. As the crack tip approaches the hole boundary, the local net section stresses increase causing the SIF to increase and, thus, the residual strength to decrease. A step-wise increase in the value of the residual strength occurred immediately after the first breakthrough due to the decrease in SIF. The stresses in net section ligament between the crack tip and the second fastener hole deceased resulting in the decreased value of the SIF. With further increase in crack length, the residual strength decreased. As the crack approached the second hole the residual strength again decreased due to the hole boundary effect.

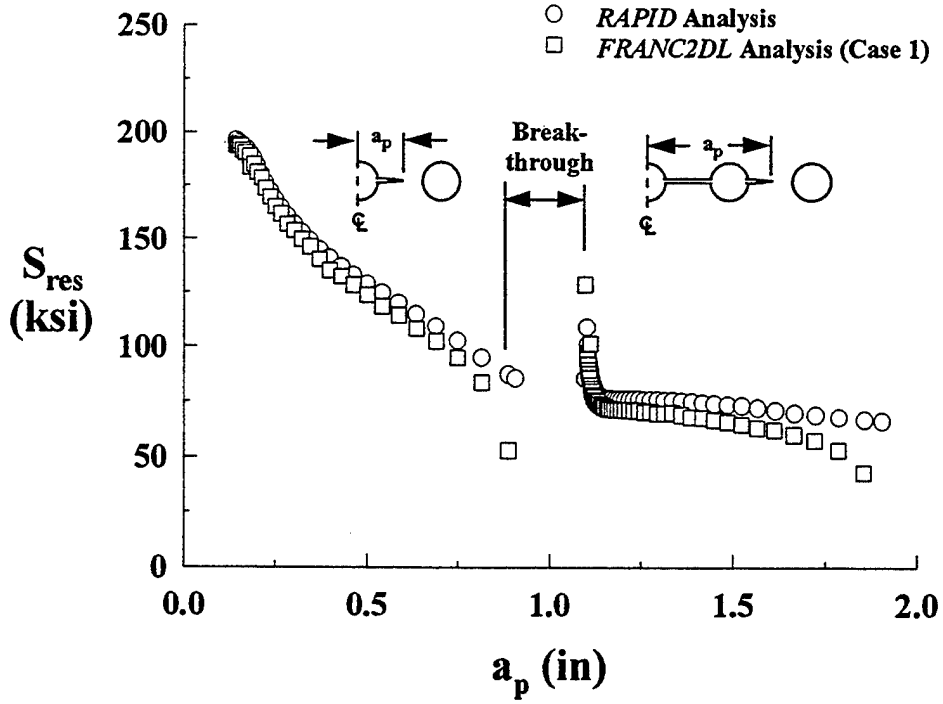

FIGURE 17. RESIDUAL STRENGTH AS A FUNCTION OF CRACK LENGTH

The differences in the residual strength shown in figure 17 are due mainly to the differences in the SIF calculated using RAPID and FRANC2DL. The largest differences occurred as the crack length approached the first and second breakthrough conditions.

INSPECTION INTERVAL.

The inspection interval as a function of the detectable crack length was determined using the ROEM approach for three repair types and compared with results generated using RAPID as shown in figures 18-20. The inspection interval, N_{ins}, was calculated using equation 9. The first data point is the inspection threshold, N_{th}, defined using equation 6. As shown in figures 18 - 20, excellent agreement was obtained between the RAPID and ROEM results up to the first breakthrough condition. The discrepancies in the results using the two methods is due to the differences in the initial flaw assumptions. In the ROEM approach, primary and secondary cracks of lengths 0.05" and 0.005", respectively, exists at both sides of the critical fastener hole and secondary cracks of length 0.005" exists on both sides of the remaining fastener holes. The growth of each crack is assumed to occur simultaneously but independently. In the RAPID analysis, the Case 2 crack growth scenario shown in figure 1 was assumed.

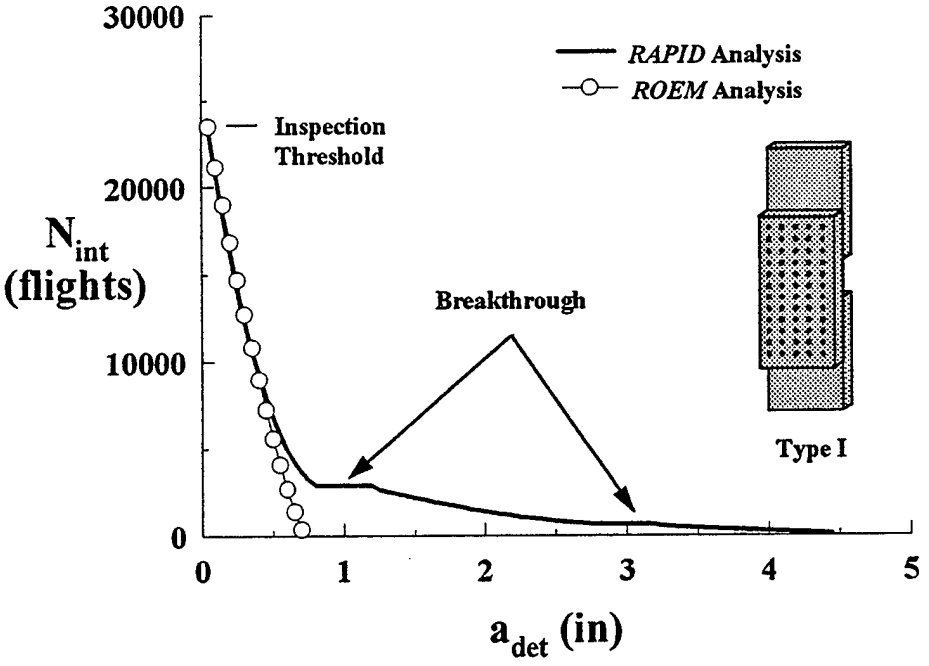

FIGURE 18. INSPECTION INTERVAL FOR REPAIR TYPE I

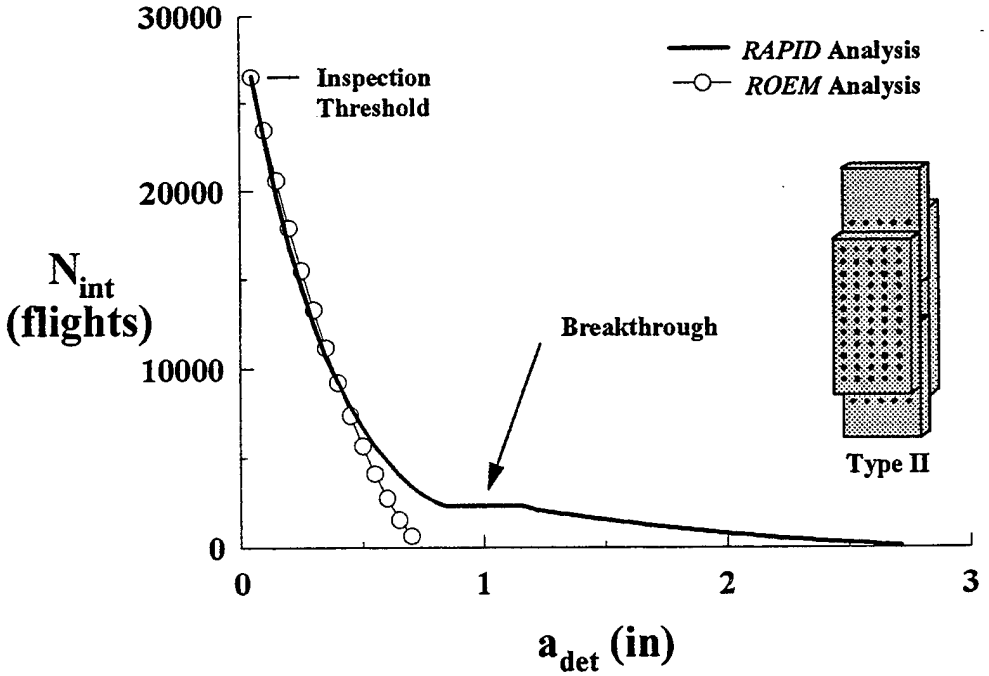

FIGURE 19. INSPECTION INTERVAL FOR REPAIR TYPE II

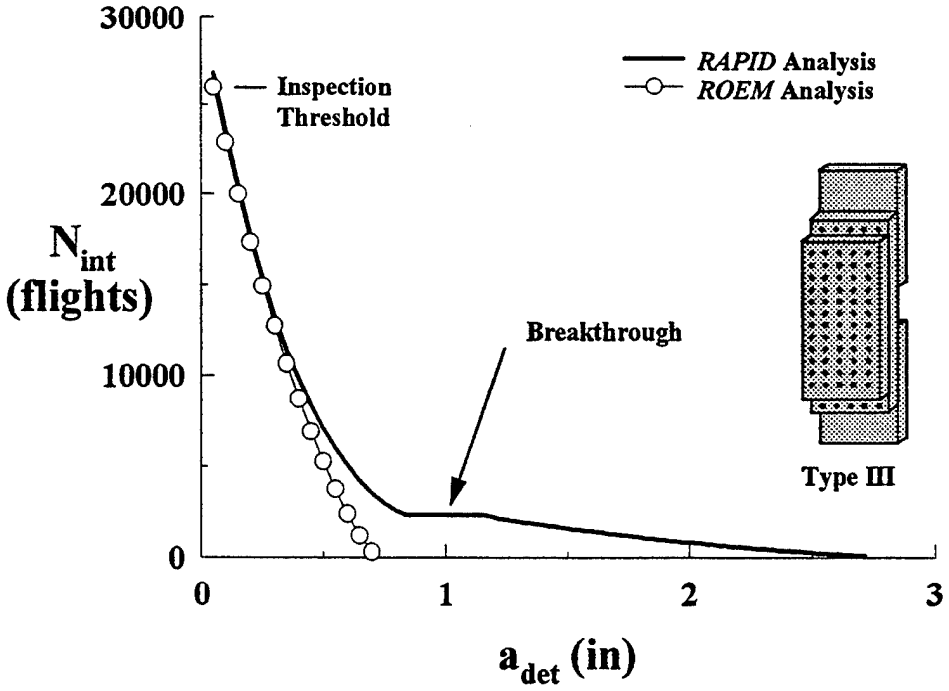

FIGURE 20. INSPECTION INTERVAL FOR REPAIR TYPE III

CONCLUDING REMARKS

In this study, the simplified damage tolerance analysis methodology in the newly developed repair software, Repair Assessment Procedure and Integrated Design (RAPID), was presented and evaluated. Results generated using RAPID compared well with results generated using a Representative Original Equipment Manufacturer (ROEM) method and a special purpose finite element program, the Fracture Analysis Code for 2-Dimensional Layered (FRANC2DL) structures. Comparisons were made in terms of the fastener loads, stress-intensity factor (SIF) solutions, crack growth, residual strength, and inspection intervals.

The fastener loads calculated using RAPID and FRANC2DL were in good agreement. There was a 1 percent difference in the value of the load at the critical fastener hole.

Trends of the SIF results calculated using RAPID and FRANC2DL were the same; the SIF values increased with crack length. As the crack tip approached the first hole, the SIF values increased substantially. The local net section stresses increase as the crack tip approaches the hole. The concentration of stress along the hole boundary causes the SIF to increase. A step-wise decrease in the value of the SIF occurred immediately after the first breakthrough. Lower stresses in the net section ligament length between the crack tip and the second fastener hole caused a decrease in the value of the SIF. The SIF values then increased with increase in crack length. There were noticeable differences in the results as the crack tip approached a hole boundary; the values of the SIF calculated using FRANC2DL were higher than those calculated using RAPID. However, this occurred over a short crack extension length.

The crack length as a function of the number of flights calculated using RAPID was compared with results using FRANC2DL. Good agreement was obtained between the RAPID and FRANC2DL results with a 8 percent difference in the number of flights to reach the first breakthrough condition. The difference in the results was due to differences in the SIF.

Both RAPID and the ROEM approach were used to calculate the crack length as a function of the number of flights for three repair types. In general, a slow crack growth process was predicted up to the first breakthrough condition for both analysis. At the first breakthrough condition, the ROEM analysis predicts sudden catastrophic fracture of the repair skin. The RAPID analysis predicts a more stable crack growth process where at least two breakthrough conditions occurred prior to catastrophic fracture of the repair skin. The difference in the results using the two methods is due to the differences in the initial flaw assumptions.

The residual strength calculations made using RAPID and FRANC2DL were in good agreement, with the largest differences occurring as the crack tip approached the fastener hole. The difference in the results was due to differences in the SIF.

Finally, the inspection interval calculated using RAPID for the three different repair types were in good agreement with results generated using the ROEM approach up to the first breakthrough condition. The difference in the results using the two methods is due to the differences in the initial flaw assumptions.

REFERENCES

1 Swift, T., "Repairs To Damage Tolerant Aircraft," *Structural Integrity of Aging Airplanes*, Eds., Atluri, S. N., Sampath, S. G., and Tong, P., pp. 433-483, July 1990.

2 Swenson, D., and James, M., "FRANC2DL: A Crack Propagation Simulator For Plane Layered Structures, Version 1.0 User's Guide," Kansas State University, December 1994.